Journal Name

ARTICLE

Effect of fluorescent staining on size measurements of polymeric nanoparticles using DLS and SAXS

D. Geißler, C. Gollwitzer, A. Sikora, C. Minelli, M. Krumrey, U. Resch-Genger

Supporting Information

The Supporting Information include:

Figure S1 exemplarily displays the comparison of fits for a measured SAXS curve assuming either solid spherical particles or core-shell particles. A core-shell model is used for SAXS data analysis, because the carboxylated polymer particles are not made of pure polystyrene (as PS does not contain any carboxylic groups), but are rather core-shell particles made up of a polystyrene core and a PMMA shell. Thus, the scattering curve can be fitted better by a core-shell model with a light core and a dense, thin shell. The visual difference between both scattering curves is rather small, especially considering the position of the first minimum which is only slightly shifted for a core-shell particle with a thin shell. However, the positions of the higher minima disagree with the assumption of solid spheres.

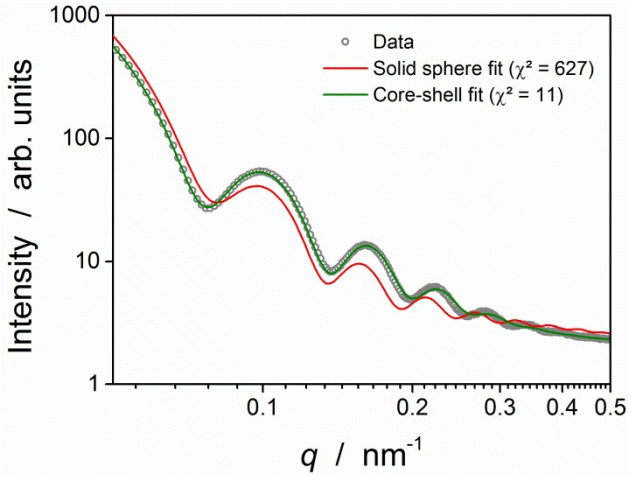

Figure S1. Comparison of the SAXS fits assuming either solid spheres or core-shell particles.

Figure S2 shows the intensity-corrected emission spectra of the dye-stained particles. The emission spectra of the DY680-stained particles displayed in Figure S2 (right) illustrate that a higher dye-staining concentration does not automatically results in a proportionally stronger emission intensity, as higher staining concentrations can induce fluorescence quenching effects due to dye-dye interactions. This becomes obvious from the emission spectrum of PS(680)-1.0, which have twice as many dyes incorporated as PS(680)-0.5 (cf. Figure 1), but clearly not a twice as intense emission.

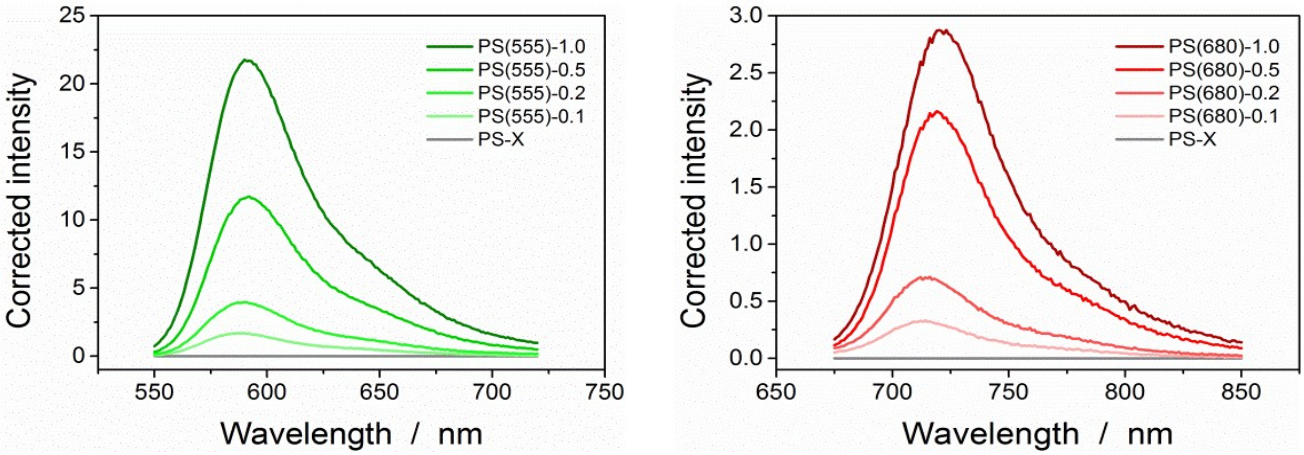

Figure S2. Intensity-corrected emission spectra of the DY555-stained (left) and DY680-stained (right) PS particles as well as the blank (unstained) control particles.

Figure S3 (left) exemplarily displays the fits for the scattering curves of the particles with the highest dye concentration. The dependency of χ2 on the particle diameter is very similar for all measured samples and is displayed in Figure S3 (right) for the two selected scattering curves. The best fit diameters (global minima) are significantly different from the mean values defined by the boundaries for which $\chi^2 > 2 \cdot \chi^2_{min}$, which means that there is a strong correlation between the particle diameter with other adjustable parameters of the model, which in turns leads to large uncertainties. Nevertheless, as the best fit diameters were for all samples within the stated uncertainties of the mean values, the mean values were used in this work (cf. Figure 3).

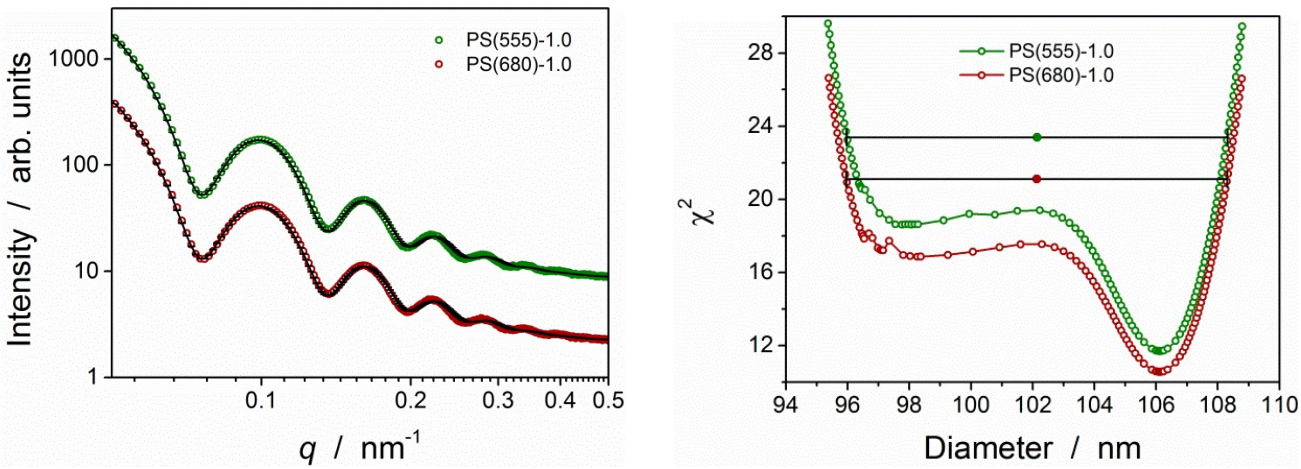

Figure S3. Model fits of the measured SAXS curves (left) and goodness-of-fit versus assumed particle diameter (right) for the polymer particles stained with 1.0 mM DY555 and DY680, i.e. PS(555)-1.0 and PS(680)-1.0, respectively.

Figure S4 displays the polydispersity (PI) values of the particle samples that (corresponding to the Z-average size values shown in Figure 4) as obtained with DLS using the cumulant fit method and two different laser excitation wavelength. As for the measure sizes there is no significant change or trend visible in the size distributions, leading to the conclusion that the size distribution is independent of the DLS device/operator, the dye absorption/laser excitation wavelength, or the dye staining concentration.

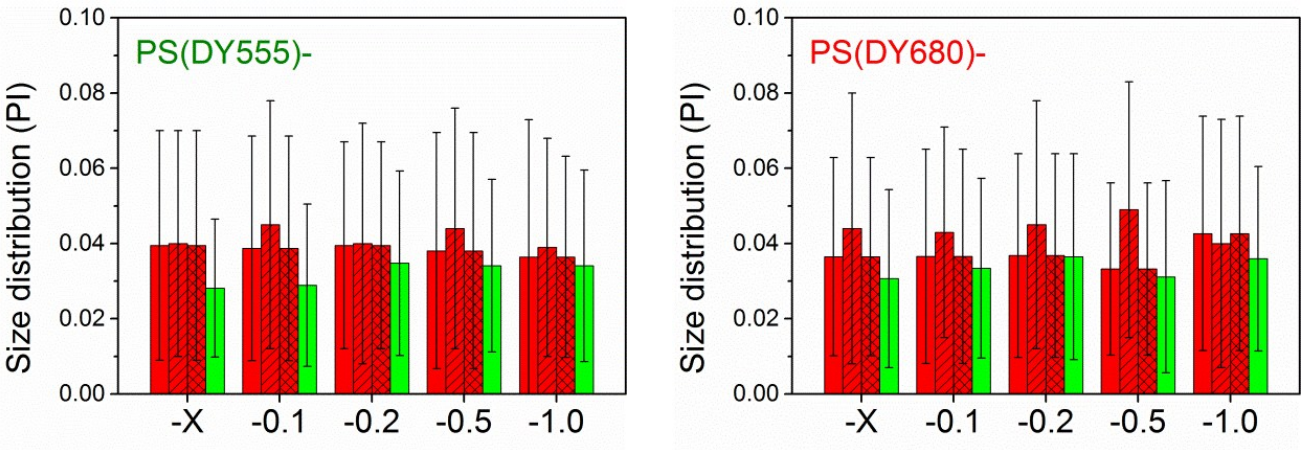

Figure S4. Size distributions (as characterized by the polydispersity index, PI) of the DY555-stained (left) and DY680-stained (right) PS particles as measured with DLS using either a "red" Zetasizer with 633 nm laser (red bars) or a "green" Zetasizer with 532 nm laser (green bars). The different textures of the red bars indicate measurements carried out at three different laboratories, and the error bars denote the standard deviations of the mean of the 100 measurements after outlier removal. The measured PI values reveal no significant effect of the dye absorption wavelength or dye staining concentration.

Figure S5 displays the number-weighted sizes and size-distributions polydispersity (PI) values of the particle samples (corresponding to the Z-average size values shown in Figure 4) as obtained with DLS applying the non-negative least square (NNLS) algorithm at two different laser excitation wavelength. As for the cumulant fit results there are no significant changes or trends visible in the size distributions, leading to the conclusion that the size distribution is independent of the DLS device/operator, the dye absorption/laser excitation wavelength, or the dye staining concentration.

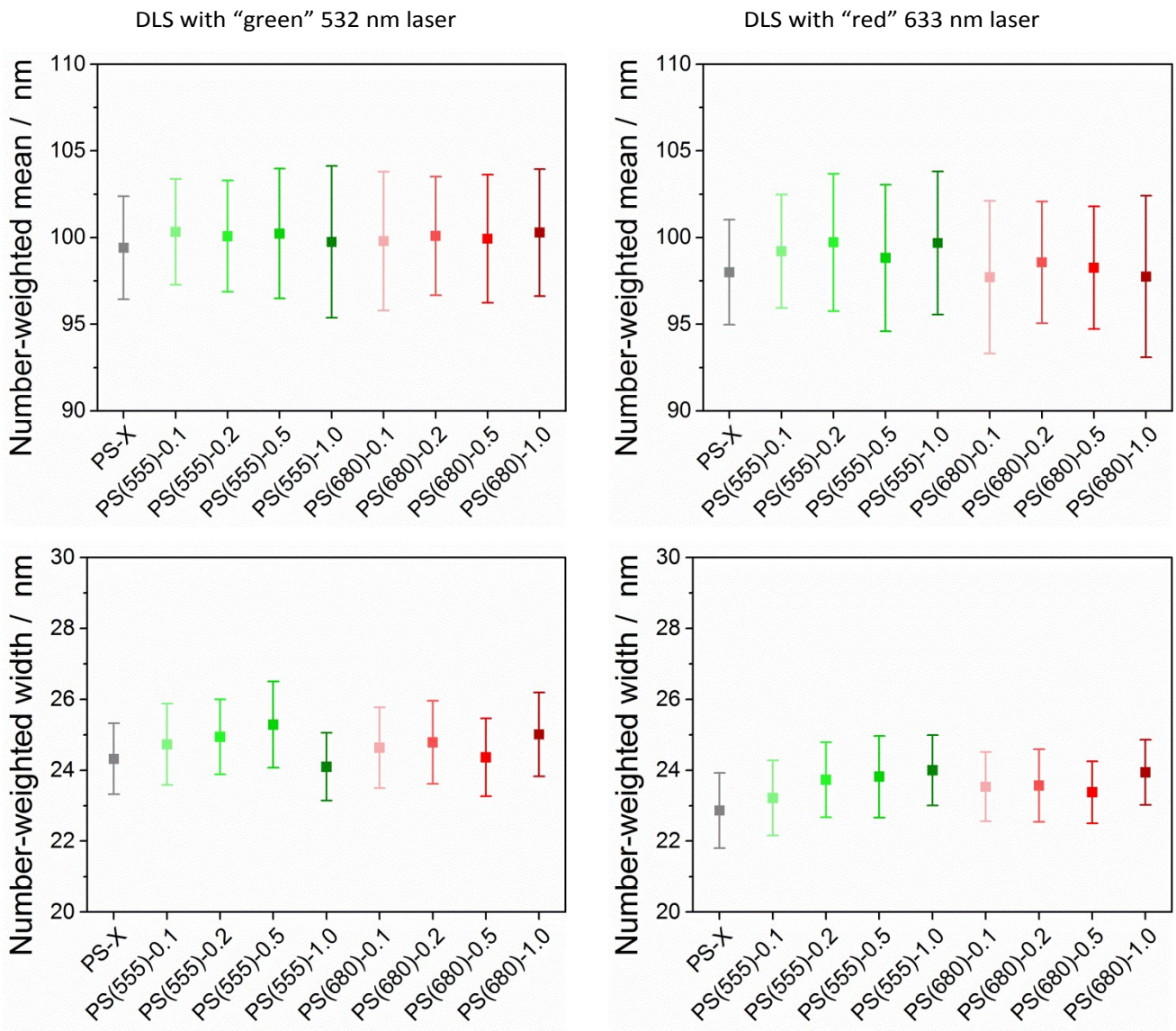

Figure S5. Number-weighted sizes (top) and size distributions (bottom) of the DY555- and DY680-stained PS particles as measured with DLS using either a “green” 532 nm laser (left) or a “red” 633 nm laser (right).